

Structure and freezing of fluids interacting via the Gay-Berne ($n-6$) potentials

Ram C. Singh,^{1,2} Jokhan Ram,¹ and Yashwant Singh¹

¹*Department of Physics, Banaras Hindu University, Varanasi 221 005, India*

²*Department of Physics, Meerut Institute of Engineering and Technology, Meerut 250 002, India*

(Received 22 August 2001; published 19 February 2002)

We have calculated the pair-correlation functions of a fluid interacting via the Gay-Berne ($n-6$) pair potentials using the Percus-Yevick integral equation theory and have shown how these correlations depend on the value of n that measures the sharpness of the repulsive core of the pair potential. These results have been used in the density-functional theory to locate the freezing transitions of these fluids. We have used two different versions of the theory known as the second order and the modified weighted-density-functional theory and examined the freezing of these fluids for $8 \leq n \leq 30$ and in the reduced temperature range lying between 0.65 and 1.25 into the nematic and the smectic A phases. For none of these cases smectic A phase was found to be stabilized though in some range of temperature for a given n it appeared as a metastable state. We have examined the variation of freezing parameters for the isotropic-nematic transition with temperature and n . We have also compared our results with simulation results wherever they are available. While we find that the density-functional theory is good to study the freezing transitions in such fluids the structural parameters found from the Percus-Yevick theory need to be improved particularly at high temperatures and lower values of n .

DOI: 10.1103/PhysRevE.65.031711

PACS number(s): 61.30.-v, 61.25.Em, 61.20.Gy

I. INTRODUCTION

In the case of nonspherical molecules the anisotropic nature of the intermolecular interactions can give rise to phases (liquid crystals) [1] that are absent when simple spherical molecules are considered. Depending upon the shape and the size of molecules and upon the external parameters (temperature, pressures, etc.) a system may show a wide variety of phenomena and transitions in between the isotropic liquid and the crystalline solid. All these phases including that of the isotropic liquid and the crystalline solids are characterized by the average positions and orientations of molecules and by the intermolecular spatial and orientational correlations. The determination of phase diagram of such a system from the intermolecular potential is one of the most challenging problems of the statistical mechanics.

The molecules of systems that exhibit liquid crystalline phases are generally large and have group of atoms with their own local features. In general it is difficult to know the true nature of the potential energy of interaction between such molecules. Attempts have, however, been made to find the potential energy of interactions between two such molecules using different approximations. One such method is to sum the interatomic or site-site potentials between atoms or between interaction sites. In another and more convenient approach one uses rigid molecules approximation in which it is assumed that the intermolecular potential energy depends only on the position of the center of mass and on their orientations. If, however, our interest is to relate the phases formed and their properties to the essential molecular factor responsible for the existence of liquid crystals, it is desirable to use a phenomenological description, either as a straightforward model unrelated to any particular physical systems or as a basis for describing by means of adjustable parameters between two molecules. Most commonly used models are hard ellipsoids of revolution, hard spherocylinders [2], cut sphere, the Kihara core model [3], and the Gay-Berne [4]

model. All these are single site models and refer to rigid molecules of cylindrical symmetry. Even for these simple models calculating the complete phase diagram is difficult.

The Gay-Berne potential, in particular, is proving to be a valuable model with which to investigate the behavior of liquid crystals in recent years using computer simulation techniques [5–7]. In this paper we consider a general Gay-Berne (GB) model with $n-6$ dependence on the shifted and scaled separation, R , between the uniaxial particles.

$$u(\hat{\mathbf{e}}_i, \hat{\mathbf{e}}_j, \hat{\mathbf{r}}) = 4\epsilon(\hat{\mathbf{e}}_i, \hat{\mathbf{e}}_j, \hat{\mathbf{r}})(R^{-n} - R^{-6}), \quad (1.1)$$

where

$$R = \frac{r - \sigma(\hat{\mathbf{e}}_i, \hat{\mathbf{e}}_j, \hat{\mathbf{r}}) + \sigma_0}{\sigma_0}. \quad (1.2)$$

While unit vectors $\hat{\mathbf{e}}_i, \hat{\mathbf{e}}_j$ indicate the orientations of symmetry axes of particles i and j , the orientation of the vector joining them is denoted by the unit vector $\hat{\mathbf{r}}$. The dependence of the contact distance on the orientations of the particles and the interparticle vector is

$$\begin{aligned} \sigma(\hat{\mathbf{e}}_i, \hat{\mathbf{e}}_j, \hat{\mathbf{r}}) \\ = \sigma_0 \left[1 - \chi \left(\frac{(\hat{\mathbf{e}}_i \cdot \hat{\mathbf{r}})^2 + (\hat{\mathbf{e}}_j \cdot \hat{\mathbf{r}})^2 - 2\chi(\hat{\mathbf{e}}_i \cdot \hat{\mathbf{r}})(\hat{\mathbf{e}}_j \cdot \hat{\mathbf{r}})(\hat{\mathbf{e}}_i \cdot \hat{\mathbf{e}}_j)}{1 - \chi^2(\hat{\mathbf{e}}_i \cdot \hat{\mathbf{e}}_j)^2} \right) \right]^{-1/2}, \end{aligned} \quad (1.3)$$

where σ_0 is the contact distance for the cross configuration ($\hat{\mathbf{e}}_i \cdot \hat{\mathbf{e}}_j = \hat{\mathbf{e}}_i \cdot \hat{\mathbf{r}} = \hat{\mathbf{e}}_j \cdot \hat{\mathbf{r}} = 0$). The parameter χ is a function of the ratio $x_0 (\equiv \sigma_e / \sigma_s)$, which is defined in terms of the contact distances when the particles are end to end (e) and side by side (s),

$$\chi = \frac{x_0^2 - 1}{x_0^2 + 1}. \quad (1.4)$$

This vanishes for a sphere and tends to the limiting value of unity for an infinitely long rod. The orientational dependence of the potential well depth is given by a product of two functions,

$$\epsilon(\hat{\mathbf{e}}_i, \hat{\mathbf{e}}_j, \hat{\mathbf{r}}) = \epsilon_0 \epsilon''(\hat{\mathbf{e}}_i, \hat{\mathbf{e}}_j) \epsilon'{}^\mu(\hat{\mathbf{e}}_i, \hat{\mathbf{e}}_j, \hat{\mathbf{r}}), \quad (1.5)$$

where the scaling parameter ϵ_0 is the well depth for the cross configuration. The first of these functions

$$\epsilon(\hat{\mathbf{e}}_i, \hat{\mathbf{e}}_j) = [1 - \chi^2(\hat{\mathbf{e}}_i \cdot \hat{\mathbf{e}}_j)^2]^{-1/2} \quad (1.6)$$

clearly favors the parallel alignment of the particles and so aids liquid crystal formation. The second function has a form analogous to $\sigma(\hat{\mathbf{e}}_i, \hat{\mathbf{e}}_j, \hat{\mathbf{r}})$, i.e.,

$$\epsilon'(\hat{\mathbf{e}}_i, \hat{\mathbf{e}}_j, \hat{\mathbf{r}}) = \left[1 - \chi' \left(\frac{(\hat{\mathbf{e}}_i \cdot \hat{\mathbf{r}})^2 + (\hat{\mathbf{e}}_j \cdot \hat{\mathbf{r}})^2 - 2\chi'(\hat{\mathbf{e}}_i \cdot \hat{\mathbf{r}})(\hat{\mathbf{e}}_j \cdot \hat{\mathbf{r}})(\hat{\mathbf{e}}_i \cdot \hat{\mathbf{e}}_j)}{1 - \chi'^2(\hat{\mathbf{e}}_i \cdot \hat{\mathbf{e}}_j)^2} \right) \right], \quad (1.7)$$

where the parameter χ' is determined by the ratio of the well depths, $k' (\equiv \epsilon_s / \epsilon_e)$, via

$$\chi' = \frac{k'^{1/\mu} - 1}{k'^{1/\mu} + 1}. \quad (1.8)$$

The potential contains four parameters (x_0, k', μ, ν) that determine the anisotropy in the repulsive and attractive forces, in addition to two parameters (σ_0, ϵ_0) that scale the distance and energy, respectively. The ratio of the end-to-end and side-by-side contact distance, x_0 , is related to the anisotropy of the repulsive forces and it also determines the difference in the depth of the attractive well between the side-by-side and the cross configurations. The parameter k' is the ratio of the well depth for the side-by-side and end-to-end configurations. While x_0 determines the ability of the system to form an orientationally ordered phase, k' determines the tendency of the system to form a smectic phase [7]. The other two parameters μ and ν influence nematic and smectic phase forming character of the anisotropic attractive forces in a more subtle way.

In almost all of the simulation and theoretical studies to date n has been taken equal to 12. The value of n defines the nature of the repulsion; the higher the value of n the harder is the nature of the repulsion. In Fig. 1 we plot $u^*(r, \Omega_1, \Omega_2) [= u(r, \Omega_1, \Omega_2) / \epsilon_0]$ as a function of separation for some fixed orientations with $n = 10$ and 18. It shows that as n increases the importance of attractive interaction increases for all orientations. In the present paper we inves-

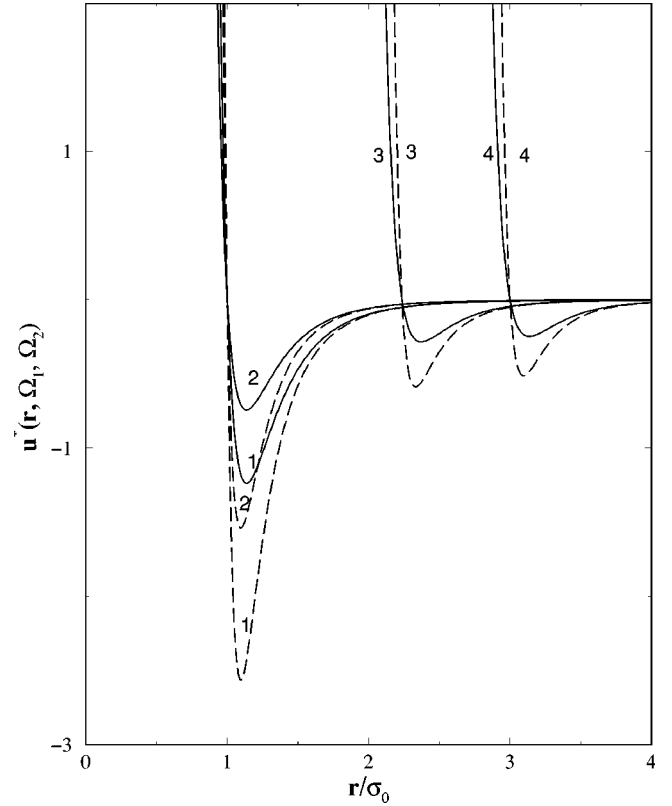


FIG. 1. Comparison of the GB($n-6$) intermolecular potential as a function of the particle separation r/σ_0 for four molecular arrangements: parallel (curve 1), cross (curve 2), T shaped (curve 3), and end to end (curve 4). Solid lines are for the (10-6) model and dashed curves are for the (18-6) model.

tigate the effect of variation of n , i.e., variation of the range of repulsion on the properties of molecular liquids and on its freezing transition.

The paper is organized as follows. In Sec. II, we describe the solution of the Ornstein-Zernike equation using the Percus-Yevick closure relation for pair-correlation functions. Section III discusses the essential details of density-functional formalism applied to study the freezing of molecular fluids into ordered phases. The results are given and discussed in Sec. IV.

II. PAIR-CORRELATION FUNCTIONS: SOLUTION OF THE PERCUS-YEVICK EQUATION

The single particle density distribution $\rho(1)$ is defined as

$$\rho(1) = \rho(\mathbf{r}, \mathbf{\Omega}) = \left\langle \sum_{i=1} \delta(\mathbf{r} - \mathbf{r}_i) \delta(\mathbf{\Omega} - \mathbf{\Omega}_i) \right\rangle, \quad (2.1)$$

where \mathbf{r}_i and $\mathbf{\Omega}_i$ give the position and the orientation of i th molecule, the angular bracket represents the ensemble average, and the δ the Dirac delta function, is constant independent of position and orientation for an isotropic fluid. It therefore contains no information about the structure of the system. The structural information of an isotropic fluid is contained in the two-particle density distribution $\rho(\mathbf{1}, \mathbf{2})$ that

gives the probability of finding simultaneously a molecule in a volume element $d\mathbf{r}_1 d\mathbf{\Omega}_1$ centered at $(\mathbf{r}_1, \mathbf{\Omega}_1)$ and a second molecule in a volume element $d\mathbf{r}_2 d\mathbf{\Omega}_2$ centered at $(\mathbf{r}_2, \mathbf{\Omega}_2)$. $\rho(\mathbf{1}, \mathbf{2})$ is defined as

$$\rho(\mathbf{1}, \mathbf{2}) \equiv \rho(\mathbf{r}_1, \mathbf{\Omega}_1; \mathbf{r}_2, \mathbf{\Omega}_2) = \left\langle \sum_{i \neq j} \delta(\mathbf{r}_1 - \mathbf{r}_i) \delta(\mathbf{\Omega}_1 - \mathbf{\Omega}_i) \delta(\mathbf{r}_2 - \mathbf{r}_j) \delta(\mathbf{\Omega}_2 - \mathbf{\Omega}_j) \right\rangle. \quad (2.2)$$

The pair-correlation function $g(\mathbf{1}, \mathbf{2})$ is related to $\rho(\mathbf{1}, \mathbf{2})$ by the relation

$$g(\mathbf{1}, \mathbf{2}) = \frac{\rho(\mathbf{1}, \mathbf{2})}{\rho(\mathbf{1})\rho(\mathbf{2})}. \quad (2.3)$$

Since for the isotropic fluid $\rho(\mathbf{1}) = \rho(\mathbf{2}) = \rho_f = \langle N \rangle / V$ where $\langle N \rangle$ is the average number of molecules in volume V ,

$$\rho_f^2 g(\mathbf{r}, \mathbf{\Omega}_1, \mathbf{\Omega}_2) = \rho(\mathbf{r}, \mathbf{\Omega}_1, \mathbf{\Omega}_2), \quad (2.4)$$

where $\mathbf{r} = (\mathbf{r}_2 - \mathbf{r}_1)$. In the isotropic phase $\rho(\mathbf{1}, \mathbf{2})$ depends only on the distance $|\mathbf{r}_2 - \mathbf{r}_1| = r$, the orientation of molecules with respect to each other and on the direction of vector $\hat{\mathbf{r}} = \mathbf{r}/r$ (a unit vector along \mathbf{r}). The pair-distribution function $g(\mathbf{1}, \mathbf{2})$ of the isotropic fluid is of particular interest as it is the lowest-order microscopic quantity that contains informations about the translational and the orientational structures of the system and also has direct contact with intermolecular (as well as with intramolecular) interactions. For an ordered phase, on the other hand, most of the structural informations are contained in $\rho(\mathbf{x})$ (see Sec. III).

The values of the pair-correlation functions as a function of intermolecular separation and orientations at a given temperature and pressure are found either by computer simulations or by solving the Ornstein-Zernike (OZ) equation

$$h(\mathbf{1}, \mathbf{2}) - c(\mathbf{1}, \mathbf{2}) = \gamma(\mathbf{1}, \mathbf{2}) = \rho_f \int c(\mathbf{1}, \mathbf{3}) [\gamma(\mathbf{2}, \mathbf{3}) + c(\mathbf{2}, \mathbf{3})] d\mathbf{3}, \quad (2.5)$$

where $d\mathbf{3} = d\mathbf{r}_3 d\mathbf{\Omega}_3$ and $h(\mathbf{1}, \mathbf{2}) = g(\mathbf{1}, \mathbf{2}) - 1$ and $c(\mathbf{1}, \mathbf{2})$ are, respectively, the total and direct pair-correlation functions, using a suitable closure relation. Most commonly used closer relations are the Percus-Yevick (PY) and the hypernetted chain (HNC) relations. Approximations are introduced through these closure relations. The PY and HNC integral equation theories are given by the OZ equation coupled with the closure relation [8]

$$C^{PY}(\mathbf{1}, \mathbf{2}) = f(\mathbf{1}, \mathbf{2}) [1 + \gamma(\mathbf{1}, \mathbf{2})] \quad (2.6)$$

and

$$C^{HNC}(\mathbf{1}, \mathbf{2}) = h(\mathbf{1}, \mathbf{2}) - \ln[1 + h(\mathbf{1}, \mathbf{2})] - \beta u(\mathbf{1}, \mathbf{2}), \quad (2.7)$$

respectively. Here $f(\mathbf{1}, \mathbf{2}) = \exp[-\beta u(\mathbf{1}, \mathbf{2})] - 1$ and $\beta = (k_B T)^{-1}$.

Both the PY and HNC integral theories have been used to find the pair-correlations functions of model fluids of non-spherical molecules [9,10]. It is found that while the PY theory underestimates the correlations, particularly the angular correlation the HNC theory overestimates them. In case of hard-core fluids we proposed a ‘‘mixed’’ integral equation that interpolates between the HNC and PY theories and is thermodynamically consistent [11]. Such an approach is needed for the soft-core potential the one considered in this paper also. We, however, defer this approach for the future and confine ourselves here to solve the PY equation to get the pair correlation functions for the GB ($n-6$) potential.

The angle dependent function $A(\mathbf{r}_{12}, \mathbf{\Omega}_1, \mathbf{\Omega}_2)$ (where A may be pair-correlation function or pair potential) is expanded in a basis set of rotational invariants [8] in space fixed (SF) frame according to the equation

$$A(\mathbf{r}_{12}, \mathbf{\Omega}_1, \mathbf{\Omega}_2) = \sum_{l_1 l_2 l} \sum_{m_1 m_2 m} A_{l_1 l_2 l}(r_{12}) \times C_g(l_1 l_2 l; m_1 m_2 m) Y_{l_1 m_1}(\mathbf{\Omega}_1) \times Y_{l_2 m_2}(\mathbf{\Omega}_2) Y_{lm}^*(\mathbf{\Omega}), \quad (2.8)$$

where $C_g(l_1 l_2 l; m_1 m_2 m)$ are the Clebsch-Gordon coefficients.

For fully axially symmetric particles it is also possible to expand the function in products of spherical harmonics in body fixed (BF) frame according to the equation.

$$A(\mathbf{r}_{12}, \mathbf{\Omega}_1, \mathbf{\Omega}_2) = \sum_{l_1 l_2 m} A_{l_1 l_2 m}(r_{12}) Y_{l_1 m}(\mathbf{\Omega}_1) Y_{l_2 m}(\mathbf{\Omega}_2), \quad (2.9)$$

where $\underline{m} \equiv -m$. Numerically it is easier to calculate the BF harmonic coefficients than the SF harmonic coefficients. The two harmonic coefficients are related through a linear transformation,

$$A_{l_1 l_2 m}(r_{12}) = \sum_l \left(\frac{2l+1}{4\pi} \right)^{1/2} A_{l_1 l_2 l}(r_{12}) C_g(l_1 l_2 l; \underline{m} m 0)$$

or

$$A_{l_1 l_2 l}(r_{12}) = \sum_m \left(\frac{4\pi}{2l+1} \right)^{1/2} A_{l_1 l_2 m}(r_{12}) C_g(l_1 l_2 l; \underline{m} m 0). \quad (2.10)$$

In any numerical calculation we can handle only a finite number of the spherical harmonic coefficients for each orientation-dependent function. The accuracy of the results depends on this number. As the anisotropy in the shape of molecules (or in interactions) and the value of fluid density ρ_f increases more harmonics are needed to get proper convergence. We have found that the series get converged if we truncate the series at the value of l indices equal to 6 for molecules with $x_0 \leq 3$ [9]. Though it is desirable to include higher-order harmonics, i.e., for $l > 6$ but it will increase computational time manifold. Our interest is to use the data of the harmonics of pair-correlation functions for freezing

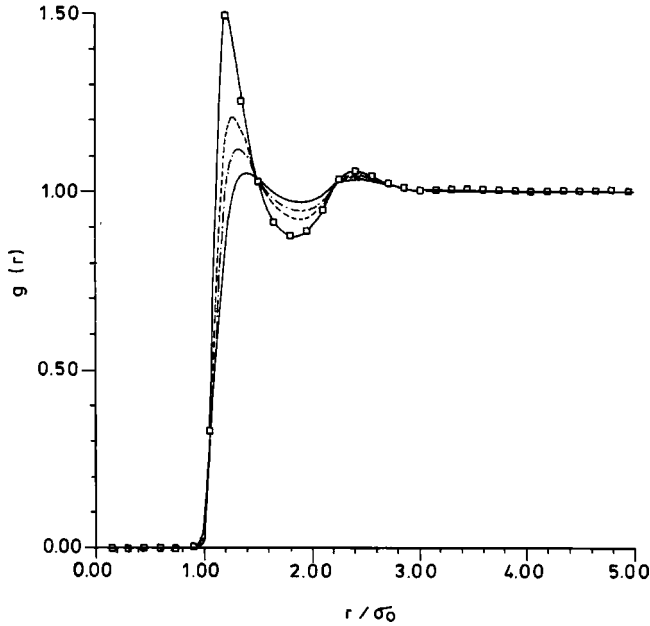


FIG. 2. Pair-correlation functions of the center of mass $g(r)$ for $x_0=3.0$, $k'=5.0$, $\eta=0.25$, and $T^*=0.80$. The solid, dash-dotted, dashed, and solid line with square curves are for (10-6), (12-6), (14-6), and (18-6) potentials, respectively.

transitions where only low-order harmonics are generally involved (see Sec. III below). The only effect the higher-order harmonics appear to have on these low-order harmonics is to modify the finer structure of the harmonics at small values of r whose contributions to the structural parameters (to be define below) are negligible.

Using the numerical procedure outlined elsewhere [9], we have solved the PY equation for the GB ($n-6$) fluid having n values 8, 10, 12, 14, 16, 18, 20, 22, 24, 26, 28, and 30 for $x_0=3.0$ and well-depth ratio $k'=5$ at reduced temperatures, $T^*=kT/\epsilon_0=0.65, 0.80, 0.95$, and 1.25 for a wide range of densities. The other two parameters μ and ν are taken to be 2 and 1, respectively. The solutions could be found only upto certain density ρ' the value of which depend upon the temperature and the value of n . The value of ρ' is often close to the isotropic-nematic transition. Because of this one faces problems in locating other less symmetric phases of the system using the theory to be discussed in Sec. III.

In Fig. 2 we compare the values of $g(r)=1+[h_{000}(r)/4\pi]$ in BF frame at $T^*=0.80$ and density $\eta[\equiv(\pi/6)\rho_f\sigma_0^3x_0]=0.25$ for four sets of ($n-6$) combinations. It is seen from this figure that the first peak becomes sharper and attains its maximum value at smaller value of $r^*(=r/\sigma_0)$ as the hardness of the core increases. The cause of this becomes clear if we look at Figs. 3 and 4 that depict $v(r)=-T^*\ln[\langle\exp[-\beta u(r,\Omega_1,\Omega_2)]\rangle_{\Omega_1,\Omega_2}]$ as a function of interparticle separation at $T^*=0.8$ and 1.25, respectively. $v(r)$ may be regarded as an averaged pair potential and, therefore, helps us in understanding the features of $g(r)$. $v(r)$ seems to have two minimum; one at $r^*\approx 1.25$ and other at $r^*\approx 2.25$. The first minimum becomes deeper at higher n and at lower temperature and almost vanishes at lower n and higher temperatures. The second minimum dependence on n

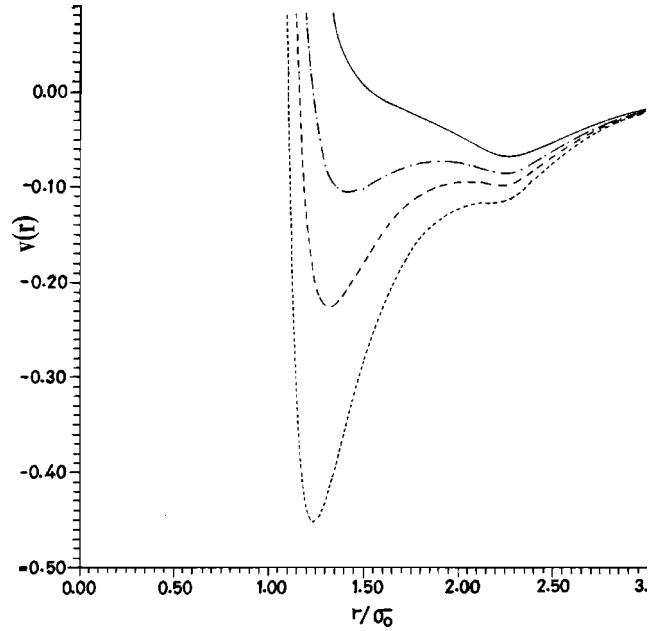


FIG. 3. The angle averaged potential $v(r)$ as a function of intermolecular separation for $x_0=3.0$, $k'=5.0$, and $T^*=0.80$. The solid, dash-dotted, dashed, and dotted curves are for (10-6), (12-6), (14-6), and (18-6) potentials, respectively.

(as well as on temperature) is weak. One may also note the shift to lower values of r^* of first minimum as n is increased.

Since the PY theory is known to be reasonably accurate for systems interacting via pair potential that has hard repul-

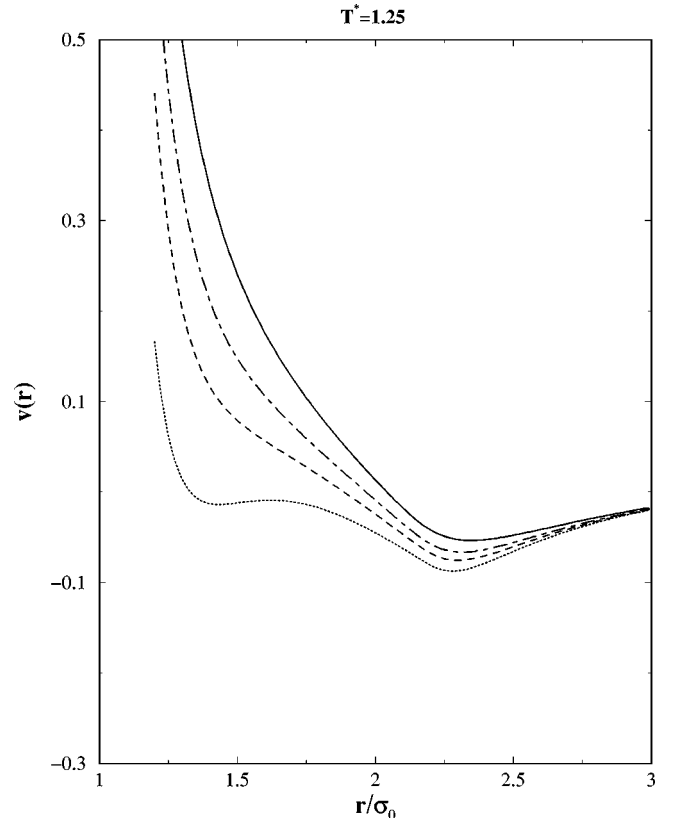


FIG. 4. Same as Fig. 3 but for $T^*=1.25$.

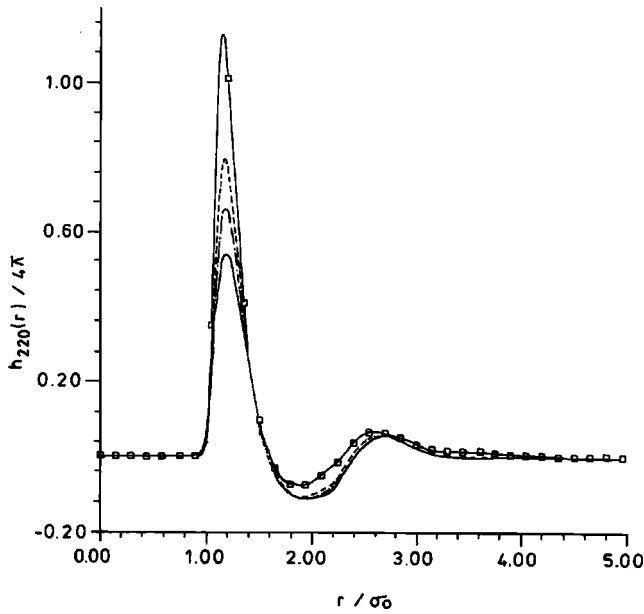


FIG. 5. The spherical harmonics coefficient $h_{220}(r)/4\pi$ in BF frame. Curves and state conditions are the same as in Fig. 2.

sive core ($n \rightarrow \infty$) and weak attraction [11], the values of the pair-correlation functions reported here are expected to be more accurate for higher values of n and lower values of T^* compared to values corresponding to lower n and higher T^* .

In Figs. 5 and 6 we compare the two other projections of pair-correlation function in BF frame at the same state conditions and observe similar behavior. In Fig. 7 we compare the value of $g(r)$ at $\eta=0.5$ for the GB (10-6) model at four different temperatures. Here we see that the first peak gets sharper as the temperature decreases. Such behavior is also seen (see Fig. 2) when n is increased at the same temperature. This is due to increasing tendency of the molecules to form parallel configurations.

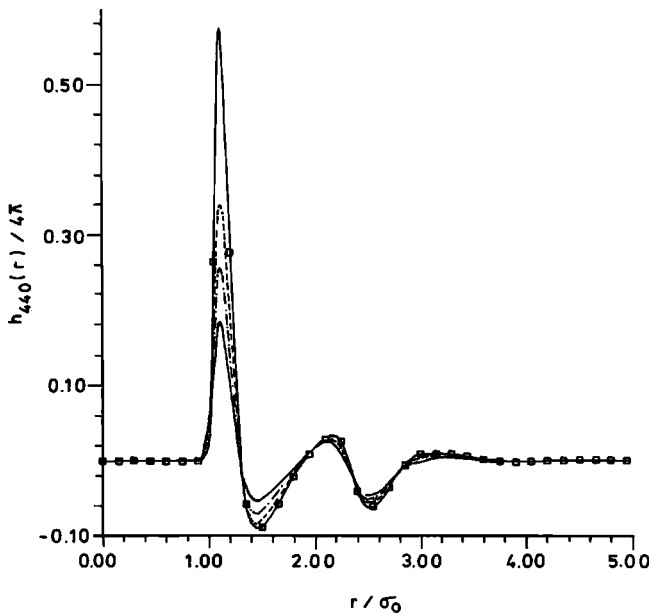


FIG. 6. The spherical harmonics coefficient $h_{440}(r)/4\pi$ in BF frame. Curves and state conditions are the same as in Fig. 2.

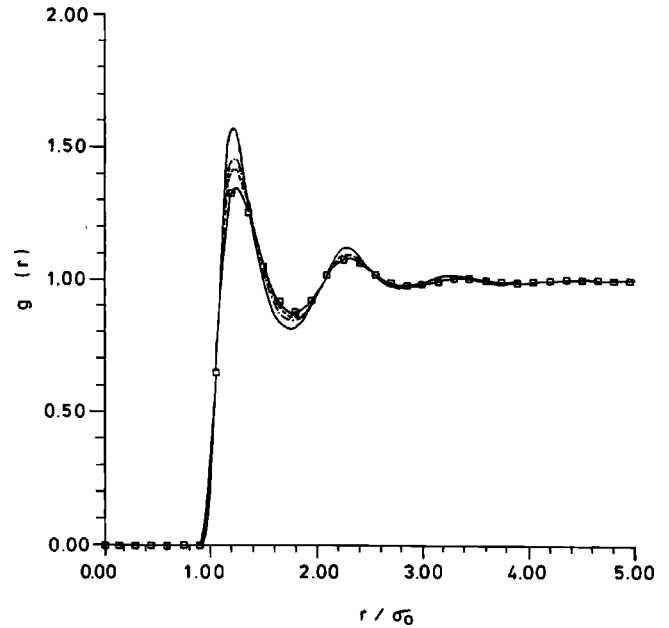


FIG. 7. Pair-correlation function of the center of mass $g(r)$ for $\eta=0.50$ for the GB (10-6) model. The solid, dash-dotted, dashed, and solid line with square are for the temperatures $T^*=0.65, 0.80, 0.95,$ and $1.25,$ respectively.

As has already been mentioned, the PY theory underestimates the molecular correlations. This can be seen from the pressure calculated using the values of the direct pair-correlation function through the compressibility relation that is found to be lower than the simulated value as shown in Fig. 8.

For a system consisting of axially symmetric nondipolar molecules the static Kerr constant K is given by [12,13]

$$K = \beta\kappa \left[1 - \frac{\hat{C}_{22}^0}{5} \right]^{-1},$$

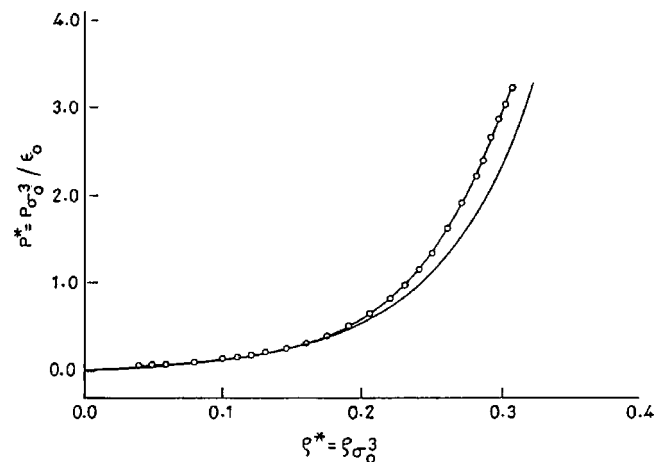


FIG. 8. Pressure as a function of fluid density for the GB (12-6) fluid at $T^*=0.95$. The solid curve is the present PY result obtained using the compressibility equation. The open circles are the MD result of Miguel *et al.* (Ref. [5]).

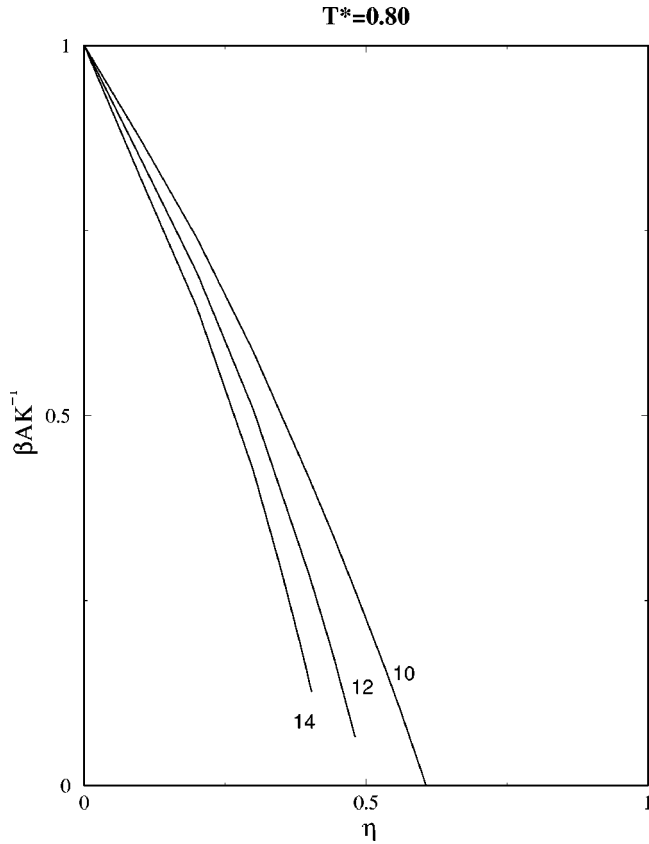


FIG. 9. The reduced inverse Kerr constant βAK^{-1} as a function of density η for $x_0 = 3.0$, $k' = 5.0$, and $T^* = 0.80$. The values of n in GB ($n-6$) models for the different curves are given on the plot.

where \hat{C}_{22}^0 is structural parameter defined as in Eq. (3.22) and κ is a constant dependent only upon single particle properties. The divergence of K may signal the absolute stability limit of the isotropic phase relative to orientationally ordered phase [12]. Thus the isotropic phase becomes orientationally unstable when the inverse Kerr constant $K^{-1} \rightarrow 0$. It is, however, important to emphasize that the condition $K^{-1} \rightarrow 0$ does not determine the thermodynamic phase transition, but rather a point on the spinodal line. This means that the density at which $K^{-1} = 0$ establishes a stability limit in the sense that at higher densities the isotropic phase cannot exist even as a metastable state.

The reduced Kerr constants βAK^{-1} as a function of η for the various n values are plotted in Figs. 9 and 10 at $T^* = 0.8$ and 1.25.

III. THEORY FOR FREEZING

The structural informations of fluids at the pair-correlation functions level obtained above can be used to obtain information about their freezing. At the freezing point the spatial and orientational configurations of molecules undergo a modification. Often abrupt change in the symmetries of the system takes place on the freezing. In contrast to the isotropic fluid, the molecular configurations of most ordered phases are adequately described by the single particle density (singlet) distribution $\rho(\mathbf{x}) \cdot \rho(\mathbf{x})$ provides us with a conve-

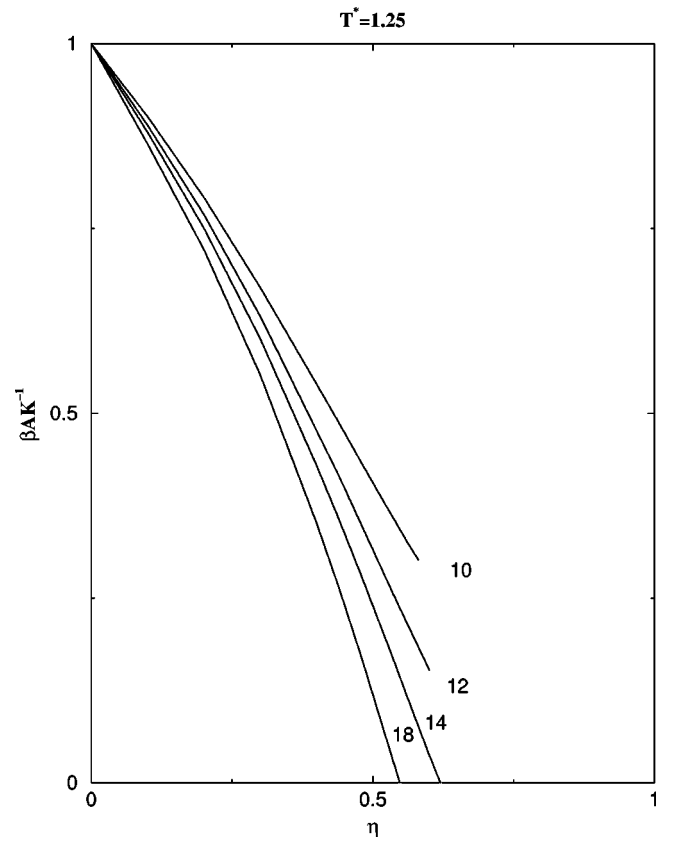


FIG. 10. Same as in Fig. 9 but for $T^* = 1.25$.

nient quantity to specify an arbitrary state of a system. One may consider a variational thermodynamic potential as a functional of $\rho(\mathbf{x})$. The equilibrium state of the system at given T and P is described by the density $\rho(T, P, \mathbf{x})$ corresponding to the minimum of the thermodynamic potential with respect to $\rho(\mathbf{x})$. This forms the basis of the density-functional theory.

In this paper we investigate the freezing of the GB($n-6$) fluid into the nematic and the smectic A (Sm A) phases using density-functional theory (DFT). In the nematic phase the full translational symmetry of the isotropic fluid phase (denoted as R^3) is maintained but the rotational symmetry $O(3)$ or $SO(3)$ (depending upon the presence or absence of the center of symmetry) is broken. In the simplest form of the axially symmetric molecules the group $O(3)$ [or $SO(3)$] is replaced by one of the uniaxial symmetry $D_{\infty h}$ (or D_{∞}). The phase possessing the $R^3 \wedge D_{\infty h}$ (denoting the semidirect product of the translational group R^3 and the rotational group $D_{\infty h}$) symmetry is known as uniaxial nematic phase [1,14].

The smectic liquid crystals, in general, have a stratified structure with the long axes of molecules parallel to each other in layers. This situation corresponds to partial breakdown of translational invariance in addition to breaking of the orientational invariance. Since a variety of molecular arrangements are possible within each layer, a number of smectic phases are possible [1]. The simplest among them is the Sm A phase. In it the center of mass of molecules in a layer are distributed as in a two-dimensional fluid but the molecular axes are on the average along a direction normal to the

smectic layer (i.e., the director \hat{n} is normal to the smectic layer). The symmetry of the Sm A phase is $D_{\infty h} \wedge (R^2 \times Z)$ where R^2 corresponds to a two-dimensional liquid structure and Z for a one-dimensional periodic structure.

The order parameters that characterize the ordered structures can be found from the singlet distribution $\rho(x)$. For this we express it in the Fourier series and the Wigner rotation matrices. Thus

$$\rho(\mathbf{x}) = \rho(\mathbf{r}, \mathbf{\Omega}) = \rho_0 \sum_q \sum_{lmn} Q_{lmn}(G_q) \exp(i\mathbf{G}_q \cdot \mathbf{r}) D_{mn}^l(\mathbf{\Omega}), \quad (3.1)$$

where the expansion coefficients

$$Q_{lmn}(G_q) = \frac{2l+1}{N} \int d\mathbf{r} \int d\mathbf{\Omega} \rho(\mathbf{r}, \mathbf{\Omega}) \exp(-i\mathbf{G}_q \cdot \mathbf{r}) D_{mn}^{l*}(\mathbf{\Omega}) \quad (3.2)$$

are the order parameters, G_q the reciprocal lattice vectors, ρ_0 the mean number density, and $D_{mn}^l(\mathbf{\Omega})$ the generalized spherical harmonics or Wigner rotation matrices [15].

Since we are interested in uniaxial systems of cylindrically symmetric molecules, $m=n=0$ in Eqs. (3.1) and (3.2). This leads to

$$\rho(\mathbf{r}, \mathbf{\Omega}) = \rho_0 \sum_l \sum_q Q_{lq} \exp(i\mathbf{G}_q \cdot \mathbf{r}) P_l(\cos \theta) \quad (3.3)$$

and

$$Q_{lq} = \frac{2l+1}{N} \int d\mathbf{r} \int d\mathbf{\Omega} \rho(\mathbf{r}, \mathbf{\Omega}) \exp(-i\mathbf{G}_q \cdot \mathbf{r}) P_l(\cos \theta), \quad (3.4)$$

where $P_l(\cos \theta)$ is the Legendre polynomial of degree l and θ is the angle between the cylindrical axis of a molecule and the director.

Since in the nematic phase the centres of mass of molecules are distributed as randomly as in the isotropic fluid but the molecular axes are aligned along a particular direction defined by the director $\hat{\mathbf{n}}$ (a unit vector) we have $G_q = 0$ and

$$Q_{l0} = \langle (2l+1) P_l[\cos(\theta)] \rangle = (2l+1) \bar{P}_l, \quad (3.5)$$

where angular bracket indicates the ensemble average. It is often enough to use two orientational order parameters \bar{P}_2 and \bar{P}_4 to locate the isotropic-nematic transition as in almost all known cases the transition is weak first-order transition [1].

To characterize the Sm A phase we need three different class of order parameters; (i) orientational, (ii) positional, (iii) mixed. These parameters are found from Eq. (3.2). For the orientational order we take \bar{P}_2 and \bar{P}_4 as in the case of the nematic phase. For the positional order along the z axis we choose one order parameter corresponding $G_z = 2\pi/d$, d being the layer spacing. Thus

$$\mu = Q_{00}(G_z) = \left\langle \cos \left(\frac{2\pi z}{d} \right) \right\rangle. \quad (3.6)$$

The coupling between the positional and orientational ordering is described by the (mixed) order parameter τ defined as

$$\tau = \frac{1}{5} Q_{20}(G_z) = \left\langle \cos \left(\frac{2\pi z}{d} \right) P_2(\cos \theta) \right\rangle. \quad (3.7)$$

We therefore choose four order parameters to describe the ordering in a Sm A phase and two for the nematic ordering. Another way of writing the trial singlet distribution corresponding to the ordered phases of our interest is

$$\rho(\mathbf{r}, \mathbf{\Omega}) = A_0 \rho_0 \exp[-\alpha(z-d)^2 - \alpha^1(z-d)^2 P_2(\cos \theta) + \lambda_2 P_2(\cos \theta) + \lambda_4 P_4(\cos \theta)], \quad (3.8)$$

where A_0 is a normalization constant, α and α^1 are associated with the formation of layer in the Sm A phase and λ_2 and λ_4 with orientational ordering. When α and α^1 are zero but λ_2 and λ_4 are nonzero the phase is nematic. In case of the isotropic fluid all the four parameters α , α^1 , λ_2 , and λ_4 are zero. If all the four parameters are nonzero the phase is Sm A. The four order parameters defined above can be found taking the expression of $\rho(\mathbf{r}, \mathbf{\Omega})$ given by Eq. (3.8). Thus

$$\mu = \frac{A_0}{d} \int_0^d dz \cos \left(\frac{2\pi z}{d} \right) \int_0^1 dx \exp(S), \quad (3.9)$$

$$\tau = \frac{A_0}{d} \int_0^d dz \cos \left(\frac{2\pi z}{d} \right) \int_0^1 dx \exp(S) P_2(x), \quad (3.10)$$

$$\bar{P}_2 = \frac{A_0}{d} \int_0^d dz \int_0^1 dx \exp(S) P_2(x), \quad (3.11)$$

$$\bar{P}_4 = \frac{A_0}{d} \int_0^d dz \int_0^1 dx \exp(S) P_4(x), \quad (3.12)$$

where $S = -\alpha(z-d)^2 - \alpha^1(z-d)^2 P_2(x) + \lambda_2 P_2(x) + \lambda_4 P_4(x)$.

A. Density-functional approach

In the usual density-functional theory approach one uses the grand thermodynamic potential to locate the transition. The grand thermodynamic potential is defined as

$$-W = \beta A - \beta \mu \int d\mathbf{x} \rho(\mathbf{x}), \quad (3.13)$$

where A is the Helmholtz free energy, μ the chemical potential, and $\rho(\mathbf{x})$ is a singlet distribution function. Equation (3.1) can be written as

$$\Delta W = W - W_f = \Delta W_1 + \Delta W_2, \quad (3.14)$$

where W_f is the grand thermodynamic potential of the isotropic fluid, and [14].

$$\frac{\Delta W_1}{N} = \frac{1}{\rho_f V} \int d\mathbf{r} d\mathbf{\Omega} \left\{ \rho(\mathbf{r}, \mathbf{\Omega}) \ln \left[\frac{\rho(\mathbf{r}, \mathbf{\Omega})}{\rho_f} \right] - \Delta \rho(\mathbf{r}, \mathbf{\Omega}) \right\} \quad (3.15)$$

and

$$\frac{\Delta W_2}{N} = - \frac{1}{2\rho_f} \int d\mathbf{r}_{12} d\mathbf{\Omega}_1 d\mathbf{\Omega}_2 \Delta \rho(\mathbf{r}_1, \mathbf{\Omega}_1) \times c(\mathbf{r}_{12}, \mathbf{\Omega}_1, \mathbf{\Omega}_2) \Delta \rho(\mathbf{r}_2, \mathbf{\Omega}_2). \quad (3.16)$$

Here $\Delta \rho(\mathbf{x}) = \rho(\mathbf{x}) - \rho_f$, where ρ_f is the density of the co-existing liquid. The ordered phase density is found by minimizing ΔW with respect to arbitrary variations in the ordered phase density subject to the constraint that corresponds to some specific features of the ordered phase. Thus,

$$\ln \frac{\rho(\mathbf{r}_1, \mathbf{\Omega}_1)}{\rho_f} = \lambda_L + \int d\mathbf{r}_2 d\mathbf{\Omega}_2 c(\mathbf{r}_{12}, \mathbf{\Omega}_1, \mathbf{\Omega}_2; \rho_f) \Delta \rho(\mathbf{r}_2, \mathbf{\Omega}_2) \quad (3.17)$$

where λ_L is Lagrange multiplier that appears in the equation because of constraint imposed on the minimization.

One attempts to find a solution of $\rho(\mathbf{x})$ of Eq. (3.17) that has the symmetry of the ordered phase. These solutions, inserted in Eq. (3.14) give the grand thermodynamic potential difference between the ordered and liquid phases. The phase with the lowest grand potential is taken as the stable phase. Phase coexistence occurs at the value of ρ_f that makes $-\Delta W/N = 0$ for the ordered and liquid phases. Substituting Eq. (3.1), into Eqs. (3.17) and (3.14) and integrating results in, respectively

$$\delta_{l'0} \delta_{q'0} + \frac{Q_{l'q'}}{2l'+1} = \frac{1}{V} \int d\mathbf{r}_1 d\mathbf{\Omega}_1 e^{-i\mathbf{G}_{q'} \cdot \mathbf{r}_1} P_{l'}(\cos \theta_1) \times \exp \left[\lambda_L + \sum_l \sum_q \frac{Q_{lq}}{2l+1} \times e^{-i\mathbf{G}_q \cdot \mathbf{r}_1} \hat{C}_{l,0}^q(\theta_1) \right] \quad (3.18)$$

and

$$- \frac{\Delta W}{N} = -\Delta \rho^* + \Delta \rho^* \hat{C}_{0,0}^0 + \frac{1}{2} \sum_{LL'} \sum_q \frac{Q_{Lq} Q_{L'q}}{(2L+1)(2L'+1)} \hat{C}_{L,L'}^q, \quad (3.19)$$

where

$$Q_{0,0} = \Delta \rho^*, \quad (3.20)$$

$$\hat{C}_{l,0}^q(\theta_1) = (2l+1) \rho_f \int d\mathbf{r}_{12} d\mathbf{\Omega}_2 c(\mathbf{r}_{12}, \mathbf{\Omega}_1, \mathbf{\Omega}_2) \times e^{i\mathbf{G}_q \cdot \mathbf{r}_{12}} P_l(\cos \theta_2), \quad (3.21)$$

$$\hat{C}_{l,l'}^q = (2l+1)(2l'+1) \rho_f \int d\mathbf{r}_{12} d\mathbf{\Omega}_1 d\mathbf{\Omega}_2 \times e^{i\mathbf{G}_q \cdot \mathbf{r}_{12}} c(\mathbf{r}_{12}, \mathbf{\Omega}_1, \mathbf{\Omega}_2) \times P_l(\cos \theta_1) P_{l'}(\cos \theta_2) \quad (3.22)$$

are the structural parameters related to the Fourier transformed direct correlation function of the fluid phase. Equation (3.18) is the expression for the order parameters. This version of the density-functional theory is known as the second-order density functional theory (SODFT) because it considers only the pair-correlation functions and neglects the higher-order correlations that might be present in the system at the transition point.

B. Modified weighted-density approximation

In another version of the density-functional approach in which higher-order correlations are included and known as modified weighted-density approximation [16], one uses the Helmholtz free energy to locate the transition. For the Helmholtz free energy we write

$$A[\rho(\mathbf{r}, \mathbf{\Omega})] = A_{id}[\rho(\mathbf{r}, \mathbf{\Omega})] + A_{ex}[\rho(\mathbf{r}, \mathbf{\Omega})], \quad (3.23)$$

where both terms in Eq. (3.23) are unique functionals of the one-particle density $\rho(\mathbf{r}, \mathbf{\Omega})$. The first term in the right-hand side of Eq. (3.23) is a nonuniform ideal gas contribution of the form

$$A_{id}[\rho(\mathbf{r}, \mathbf{\Omega})] = \beta^{-1} \int_V d\mathbf{r} d\mathbf{\Omega} \rho(\mathbf{r}, \mathbf{\Omega}) \{ \ln[\rho(\mathbf{r}, \mathbf{\Omega}) \lambda^3] - 1 \}, \quad (3.24)$$

where λ is the thermal de Broglie wavelength. The second term in the right-hand side of Eq. (3.23) is the excess Helmholtz free energy of the nonuniform system.

In the modified weighted-density approximation (MWDA) the excess free energy of a uniform system, but evaluated of a weighted density $\hat{\rho}$ [16]

$$A_{ex}^{MWDA}[\rho] = N \phi_0(\hat{\rho}), \quad (3.25)$$

where N is the number of particles in the system $\phi_0(\rho)$ is the excess free energy per particle of a uniform system at density ρ . The weighted density $\hat{\rho}$ is constructed from the actual inhomogeneous one-particle density $\rho(\mathbf{x})$ and is defined by

$$\hat{\rho} = \frac{1}{N} \int_V d\mathbf{x} \rho(\mathbf{x}) \int_V d\mathbf{x}' \rho(\mathbf{x}') \tilde{\omega}(\mathbf{x} - \mathbf{x}'; \hat{\rho}), \quad (3.26)$$

introducing thereby the weighted function $\tilde{\omega}(\mathbf{x} - \mathbf{x}'; \hat{\rho})$. It is an essential ingredient of the MWDA that the weighted function $\tilde{\omega}$ that is used to determine the weighted density, de-

TABLE I. Values of order parameters and energy of smectic A and nematic phases at $T^*=0.8$ for the GB (12-6) potential. While nematic is a stable phase, smectic A is metastable as its energy is higher than the nematic.

ρ_f^*	Phase	μ_z	\bar{P}_2	\bar{P}_4	τ_{2z}	$\Delta\rho^*$	ΔW
0.293	Sm A	0.674	0.891	0.719	0.687	0.098	-0.023
	Nematic	0.000	0.843	0.562	0.000	0.058	-0.093
0.306	Sm A	0.647	0.888	0.741	0.677	0.088	-0.157
	Nematic	0.000	0.903	0.654	0.000	0.063	-0.243
0.312	Sm A	0.629	0.887	0.750	0.667	0.083	-0.234
	Nematic	0.000	0.923	0.691	0.000	0.065	-0.333

pends itself on the sought function $\hat{\rho}$; thus Eq. (3.26) has to be viewed as a self-consistency condition for the determination of the weighted density. To ensure that the approximation in the determination of $\hat{\rho}$ becomes exact in the uniform limit, the weighted function has to be normalized, i.e.,

$$\int d\mathbf{x}\tilde{\omega}(\mathbf{x}-\mathbf{x}';\hat{\rho})=1 \quad (3.27)$$

for any $\hat{\rho}$. The function $\tilde{\omega}$ can be then uniquely specified by requiring that the approximate functional $A_{ex}^{MWDA}[\rho]$ is exact upto second order in the functional expansion, namely,

$$C(\mathbf{x}-\mathbf{x}';\rho_0)=-\beta\lim_{\rho\rightarrow\rho_0}\left[\frac{\delta^2 A_{ex}^{MWDA}[\rho]}{\delta\rho(\mathbf{x})\delta\rho(\mathbf{x}')}\right]. \quad (3.28)$$

The conditions [Eqs. (3.25)–(3.28)] result in a particularly simple expression for $\tilde{\omega}$, namely,

$$\tilde{\omega}(\mathbf{x}-\mathbf{x}';\hat{\rho})=-\frac{1}{2\phi_0'(\hat{\rho})}\left[\beta^{-1}C(\mathbf{x}-\mathbf{x}';\hat{\rho})+\frac{1}{V}\hat{\rho}\phi_0''(\hat{\rho})\right], \quad (3.29)$$

where V is the volume of the sample, $\phi_0(\hat{\rho})$ is the excess free energy per particle of an isotropic fluid of density $\hat{\rho}$, and primes on $\phi_0(\hat{\rho})$ indicate derivatives with respect to density. Using expansion [Eq. (3.1)] and [Eq. (2.8)], respectively for $\rho(\mathbf{x})$ and $C(\mathbf{x}-\mathbf{x}';\hat{\rho})$ we find for the ordered phase

$$\hat{\rho}=\rho_0\sum_{L_1}\sum_{L_2}\sum_q Q_{L_1q}Q_{L_2q}\frac{\hat{c}_{L_1L_2}^q}{(2L_1+1)(2L_2+1)}\times\left[-\frac{1}{2\hat{\rho}\beta\phi_0'(\hat{\rho})}\right]-\rho_0\hat{\rho}\frac{\phi_0''(\hat{\rho})}{2\phi_0'(\hat{\rho})}. \quad (3.30)$$

Having computed $\hat{\rho}$, the next step in freezing analysis is to substitute $\hat{\rho}$ into Eq. (3.25) to compute A_{ex}^{MWDA} . In terms of structural parameter, the excess free energy per particle of a uniform system at a density ρ is given as

$$\beta\phi_0(\rho)=-\int_0^\rho d\rho''\frac{1}{\rho''2}\int_0^{\rho''}\hat{C}_{00}^0[\rho']d\rho'. \quad (3.31)$$

The ideal gas part is calculated using the ansatz for $\rho(\mathbf{r},\mathbf{\Omega})$ given by Eq. (3.8). Thus

$$\beta A_{id}[\rho_0]=\rho_0\int d\mathbf{r}\sum_L\sum_q\frac{Q_{Lq}}{\sqrt{2L+1}}e^{i\mathbf{G}_q\cdot\mathbf{r}}\times\left[\{\ln(A_0\rho_0\lambda^3)-1\}\delta_{L0}-\alpha(z-x_0)^2\frac{\delta_{2L}}{\sqrt{5}}+\frac{\lambda_2\delta_{2L}}{\sqrt{5}}+\frac{\lambda_4\delta_{4L}}{3}-\alpha^1(z-x_0)^2\delta_{L0}\right]. \quad (3.32)$$

To determine the transition parameters, we first compute the effective density $\hat{\rho}$ from Eq. (3.30) and minimizing the free energy from Eqs. (3.23), (3.31), and (3.32) with respect to $\rho_0, \alpha, \lambda_2, \lambda_4$, and α^1 . In order to determine the transition density of the coexisting isotropic (ρ_f) and anisotropic (ρ_0)

TABLE II. Isotropic-nematic transition parameters for GB ($n-6$) fluid at $T^*=0.65$. The reduced units are $P^*=P\sigma_0^3/\epsilon_0$, $\mu^*=\mu/\epsilon_0$, and $\rho^*=\rho\sigma_0^3$.

Potential model	Theory	ρ_f^*	ρ_n^*	$\Delta\rho^*$	\bar{P}_2	\bar{P}_4	P^*	μ^*
(8-6)	DFT	0.428	0.431	0.006	0.69	0.40	9.48	26.79
	MWDA	0.412	0.416	0.009	0.56	0.27	7.77	22.71
(10-6)	DFT	0.29	0.301	0.038	0.72	0.41	1.30	3.96
	MWDA	0.286	0.29	0.013	0.36	0.12	1.22	3.69

TABLE III. Same as in Table II but at $T^*=0.80$.

Potential model	Theory	ρ_f^*	ρ_n^*	$\Delta\rho^*$	\bar{P}_2	\bar{P}_4	P^*	μ^*
(10-6)	DFT	0.341	0.346	0.015	0.68	0.37	3.81	12.44
	MWDA	0.339	0.341	0.007	0.40	0.15	3.71	12.16
(12-6)	DFT	0.282	0.295	0.046	0.74	0.43	1.38	4.11
	MWDA	0.277	0.281	0.015	0.36	0.12	1.27	3.69
(14-6)	DFT	0.239	0.277	0.158	0.92	0.62	0.58	0.65
	MWDA	0.237	0.241	0.019	0.27	0.08	0.55	0.54

phases it is necessary to equate the pressure and chemical potentials (Maxwell construction) of the two phases.

IV. RESULTS AND DISCUSSION

We have used both versions of the density-functional methods described above to locate the freezing transitions and calculate the values of the freezing parameters. The structural parameters defined by Eq. (3.22) that appear in the density-functional theory as the input data are obtained from the harmonics of the direct pair-correlation functions evaluated using the PY integral equation theory (given in Sec. II). Using these values of the structural parameters and the four order parameters $\bar{P}_2, \bar{P}_4, \mu$, and τ we have solved Eqs. (3.18) and (3.19) of the SODFT and Eqs. (3.23)–(3.32) of the MWDA for the GB ($n-6$) fluid with $8 \leq n \leq 30$ for temperatures lying between 0.65 to 1.25. All our results correspond to $\mu=2$, $\nu=1$, $x_0=3$, and $k'=5$.

Our results show that for none of the cases studied here Sm A phase gets stabilized. In the low temperature region for a given n it, however, appeared as a metastable state having free energy lower than that of the isotropic phase but higher than the nematic (see Table I). Since we have not included Sm B and crystalline phases in our investigation for the reason already given, we found only the isotropic-nematic transition.

For each n we found a lower cutoff of the temperature for the existence of the nematic phase. The nematic phase was not found to exist below this temperature. The lower cutoff temperature for the nematic phase is found to increase with n . For example, where for $n=8$ and 10 we found the nematic phase to exist at $T^*=0.65$ but not for $n \geq 12$. The computer simulation results of Miguel *et al.* [5] show that for $n=12$

the cutoff temperature is slightly above $T^*=0.8$. Our results, however, show that the nematic phase exists at $T^*=0.8$. This may be due to error in the structural parameters values found from the PY theory.

Both versions of the density-functional theory give similar results for the transition density ρ_f^* but give the values of the order parameters including the change in density at the transition that are different from each other. More surprising is the way the values of the order parameters \bar{P}_2 and \bar{P}_4 vary with temperature and with n (see Tables II–V) found from the two version of the theory. While the SODFT predicts that \bar{P}_2 and \bar{P}_4 decrease as the transition temperature is increased, the MWDA predicts them to increase. The computer simulation results [5,6] do not give any clear indication as how these parameters vary with transition temperature. Similar difference in the variation of the values of the order parameters with n is also found.

In Tables II–V we give the values of the transition parameters found from the two theories. We also give the results found from the computer simulations at $T^*=0.95$ and 1.25 for $n=12$. There is very good agreement between these results at $T^*=0.95$. The transition density found from the theories are identical though somewhat higher than the value found from the simulation. The value of $\Delta\rho^*$ found from these methods are also in good agreement, though MWDA predicts the value of $\Delta\rho^*$ that is lower than the SODFT as well as simulation value. Pressure and chemical potentials are in good agreement. But there is difference in the value of \bar{P}_2 and \bar{P}_4 . At $T^*=1.25$ both theories predict the transition density that is high compared to the molecular dynamics (MD) value. One of the possible reasons for this is, as pointed out in Sec. II, the inaccuracy in the values of c har-

TABLE IV. Same as in Table II but at $T^*=0.95$.

Potential model	Theory	ρ_f^*	ρ_n^*	$\Delta\rho^*$	\bar{P}_2	\bar{P}_4	P^*	μ^*
(10-6)	DFT	0.381	0.385	0.009	0.68	0.38	8.26	25.63
	MWDA	0.379	0.382	0.007	0.46	0.20	8.04	25.04
(12-6)	MD	0.308	0.314	0.019	0.50		3.50	12.70
	DFT	0.322	0.328	0.02	0.67	0.37	3.40	11.28
	MWDA	0.322	0.325	0.008	0.37	0.13	3.40	11.28
(14-6)	DFT	0.287	0.299	0.042	0.74	0.43	1.82	5.66
	MWDA	0.283	0.288	0.017	0.37	0.12	1.69	5.21
(16-6)	DFT	0.261	0.283	0.085	0.82	0.51	1.06	2.59
	MWDA	0.245	0.251	0.027	0.36	0.12	0.82	1.64

TABLE V. Same as in Table II but at $T^* = 1.25$.

Potential model	Theory	ρ_f^*	ρ_n^*	$\Delta\rho^*$	\bar{P}_2	\bar{P}_4	P^*	μ^*
(10-6) ^a	DFT	0.454	0.456	0.005	0.72	0.44	26.93	72.59
	MWDA	0.435	0.437	0.005	0.62	0.30	21.26	59.84
(12-6)	MD [5]	0.323	0.331	0.025	0.50		5.70	20.90
	DFT	0.378	0.382	0.009	0.68	0.38	10.90	34.27
(14-6)	MWDA	0.375	0.378	0.007	0.47	0.21	10.42	32.99
	DFT	0.344	0.349	0.014	0.68	0.38	6.57	21.88
(18-6)	MWDA	0.343	0.346	0.009	0.44	0.20	6.52	21.71
	DFT	0.306	0.315	0.028	0.72	0.41	3.43	11.52
(24-6)	MWDA	0.303	0.307	0.014	0.41	0.18	3.25	10.95
	DFT	0.273	0.291	0.065	0.79	0.49	1.81	5.35
(30-6)	MWDA	0.267	0.274	0.026	0.37	0.13	1.65	4.78
	DFT	0.249	0.283	0.137	0.90	0.61	1.11	2.38
	MWDA	0.242	0.248	0.027	0.34	0.11	0.99	1.90

^aThe results have been found by extrapolating the data of the structural parameters to high densities. The value of the transition parameters may, therefore, not be as accurate as for the other cases.

monics at higher temperature. The PY theory is known to underestimate the angular correlations and this defect of the PY theory becomes more pronounced as temperature is increased for a given n . This may be the reason why the theory predicts the transition at higher density than the MD value. As a consequence of this the transition pressure and the chemical potential are also substantially higher than the MD values. This comparison at $T^* = 0.95$ and 1.25 show that while the DFT is good to predict the freezing parameters, the PY values of structural parameters at higher temperature are lower than the actual values.

We hope to combine the PY and HNC theories to generate accurate values of the harmonics of the pair-correlation functions and with these values to compute the full phase diagram.

ACKNOWLEDGMENTS

The work was supported by the Department of Science and Technology (India) through a project grant. One of us (R.C.S.) thanks the Director and Management for providing some computational facilities at MIET.

-
- [1] P. G. de Gennes and J. Prost, *The Physics of Liquid Crystals* (Clarendon, Oxford, 1993).
- [2] D. Frenkel, *J. Phys. Chem.* **91**, 4912 (1987); **92**, 3280 (1988).
- [3] T. Kihara, *Intermolecular Forces* (Wiley, New York, 1976).
- [4] J.G. Gay and B.J. Berne, *J. Chem. Phys.* **74**, 3316 (1981).
- [5] E.D. Miguel, L.F. Rull, M.K. Chalam, K.E. Gubbins, and E.V. Swol, *Mol. Phys.* **72**, 593 (1991).
- [6] E.D. Miguel, L.F. Rull, M.K. Chalam, and K.E. Gubbins, *Mol. Phys.* **74**, 405 (1991).
- [7] M.A. Bates and G.R. Luckhurst, *J. Chem. Phys.* **110**, 7087 (1999).
- [8] J.P. Hansen and I.R. McDonald, *Theory of Simple Liquids* (Academic Press, London, 1976); C.G. Gray and K.E. Gubbins, *Theory of Molecular Fluids* (Clarendon, Oxford, 1984), Vol. 1.
- [9] J. Ram and Y. Singh, *Phys. Rev. A* **44**, 3718 (1991); J. Ram, R.C. Singh, and Y. Singh, *Phys. Rev. E* **49**, 5117 (1994).
- [10] A. Perera, P.G. Kusalik, and G.N. Patey, *J. Chem. Phys.* **87**, 1295 (1987).
- [11] R.C. Singh, J. Ram, and Y. Singh, *Phys. Rev. E* **54**, 977 (1996).
- [12] A. Perera, P.G. Kusalik, and G.N. Patey, *Mol. Phys.* **60**, 77 (1987).
- [13] S. Kielich, *Dielectric and Related Molecular Process* (Chemical Society of London, London, 1972), Vol. 1, Chap. 7.
- [14] Y. Singh, *Phys. Rep.* **207**, 351 (1991).
- [15] M.E. Rose, *Elementary Theory of Angular Momentum* (Wiley, New York, 1957).
- [16] A.R. Denton and N.W. Ashcroft, *Phys. Rev. A* **39**, 426 (1989); **39**, 4701 (1989).